Cell Reports
Report

Cell PRESS
Open ACCESS

H/ACA Small RNA Dysfunctions in Disease Reveal Key Roles for Noncoding RNA Modifications in Hematopoietic Stem Cell Differentiation

Cristian Bellodi,[1,5] Mary McMahon,[1,5] Adrian Contreras,[1] Dayle Juliano,[1] Noam Kopmar,[1] Tomoka Nakamura,[4] David Maltby,[2] Alma Burlingame,[2] Sharon A. Savage,[3] Akiko Shimamura,[4] and Davide Ruggero[1,*]
[1]School of Medicine and Department of Urology, UCSF Helen Diller Comprehensive Cancer Center, San Francisco, CA 94115, USA
[2]Department of Pharmaceutical Chemistry, University of California, San Francisco, San Francisco, CA 94143, USA
[3]Clinical Genetics Branch, Division of Cancer Epidemiology and Genetics, National Cancer Institute, Rockville, MD 20892, USA
[4]Fred Hutchinson Cancer Research Center, Seattle Children's Hospital and University of Washington, Seattle, WA 98105, USA
[5]These authors contributed equally to this work
*Correspondence: davide.ruggero@ucsf.edu
http://dx.doi.org/10.1016/j.celrep.2013.04.030

SUMMARY

Noncoding RNAs control critical cellular processes, although their contribution to disease remains largely unexplored. Dyskerin associates with hundreds of H/ACA small RNAs to generate a multitude of functionally distinct ribonucleoproteins (RNPs). The *DKC1* gene, encoding dyskerin, is mutated in the multisystem disorder X-linked dyskeratosis congenita (X-DC). A central question is whether *DKC1* mutations affect the stability of H/ACA RNPs, including those modifying ribosomal RNA (rRNA). We carried out comprehensive profiling of dyskerin-associated H/ACA RNPs, revealing remarkable heterogeneity in the expression and function of subsets of H/ACA small RNAs in X-DC patient cells. Using a mass spectrometry approach, we uncovered single-nucleotide perturbations in dyskerin-guided rRNA modifications, providing functional readouts of small RNA dysfunction in X-DC. In addition, we identified that, strikingly, the catalytic activity of dyskerin is required for accurate hematopoietic stem cell differentiation. Altogether, these findings reveal that small noncoding RNA dysfunctions may contribute to the pleiotropic manifestation of human disease.

INTRODUCTION

H/ACA small RNAs are an evolutionarily conserved class of abundant noncoding RNAs (ncRNAs) involved in a diverse range of processes including posttranscriptional modifications of functional RNAs, preribosomal RNA processing, and telomere maintenance (Baxter-Roshek et al., 2007; Lestrade and Weber, 2006; Matera et al., 2007; Reichow et al., 2007; Williams and Farzaneh, 2012). A central protein associated with all classes of H/ACA small RNAs is dyskerin, which is thereby at the nexus of controlling many diverse cellular processes (Lafontaine et al., 1998; Montanaro, 2010; Watkins et al., 1998). The largest subgroup of dyskerin-associated H/ACA small RNAs are small nucleolar RNAs (snoRNAs) that are responsible for modifying hundreds of specific nucleotides on the ribosome. The association of dyskerin with H/ACA snoRNAs is important for their stability and forms catalytically active ribonucleoprotein (RNP) complexes, which guide the site-specific conversion of uridine to pseudouridine (Ψ) residues on ribosomal RNA (rRNA) (Charette and Gray, 2000).

Importantly, the *DKC1* gene encoding dyskerin is mutated in a number of cancers and inherited human syndromes including X-linked dyskeratosis congenita (X-DC) and the clinically severe variant of dyskeratosis congenita (DC) known as Hoyeraal-Hreidarsson syndrome (Bellodi et al., 2010b; Cerami et al., 2012; Forbes et al., 2011; Heiss et al., 1998; Knight et al., 1999; Yip et al., 2012). These human syndromes are characterized by a wide range of defects including hematopoietic and cutaneous abnormalities (abnormal pigmentation, nail dysplasia, leukoplakia), increased risk of cancer, pulmonary fibrosis, and liver disease, as well as severe congenital birth defects in brain development, growth, and the genitourinary system (Kirwan and Dokal, 2008). Among all H/ACA small RNAs, the telomerase RNA (TERC) is the most characterized and is widely employed as a prognostic molecular marker of DC (Alter et al., 2007; Mitchell et al., 1999). It remains largely unknown whether a multitude of small RNAs may be affected in human disease as a consequence of mutations in *DKC1*. In addition, a central unresolved question is whether the enzymatic activity of dyskerin is perturbed in and may contribute to some of the pathological features of diseases associated with mutations in *DKC1*. Interestingly, emerging evidence further suggests that specific subsets of dyskerin-associated H/ACA snoRNAs are deregulated in hematological disorders such as leukemia, lymphoma, and multiple myeloma (Ronchetti et al., 2012; Teittinen et al., 2013; Valleron et al., 2012a, 2012b).

Here, we sought to determine the landscape of H/ACA small RNA dysregulation in patients harboring *DKC1* mutations that may underlie the wide range of pathological features observed. Surprisingly, by carrying out an extensive profiling screen for these small RNAs, we observed unexpected heterogeneity in

their expression levels in X-DC patient cells harboring distinct *DKC1* mutations. Thereby, these findings reveal unexpected complexity in the manifestation of impairments in small RNAs that may reflect an important genotype-to-phenotype relationship associated with human disease etiology. Strikingly, by applying a highly quantitative mass spectrometry approach, we identified reductions in site-specific rRNA Ψ modifications, which correspond to the decreased expression of H/ACA snoRNAs guiding the modification of these residues. Thereby, the catalytic activity of RNP complexes is also directly affected in X-DC human disease. Furthermore, we uncovered a critical role for dyskerin's catalytic activity toward hematopoietic differentiation. Altogether, these findings provide compelling evidence that the deregulated expression and function of H/ACA snoRNPs may underlie specific pathological features of human disease. Moreover, complex deregulations in the patterns of H/ACA small RNA expression may serve as important molecular markers of human health and disease.

RESULTS

Heterogeneous Defects in All Classes of H/ACA Small RNAs Are Present in X-DC Patients Harboring Distinct *DKC1* Mutations

To uncover whether *DKC1* mutations affect functionally unique subsets of dyskerin-containing H/ACA small RNPs, we undertook a systematic expression analysis to examine a large panel of H/ACA small RNAs. First, we sought to examine the expression profiles of these small RNAs directly in highly purified $CD34^+$ hematopoietic progenitor cells, as a common pathological feature and cause of lethality in X-DC patients is bone marrow failure (Dokal, 2011). To this end, we characterized patient cells harboring a mutation in the *DKC1* promoter, a C-to-G substitution at position −141 hereafter referred to as *DKC1*(c.−141 C>G) (Figure 1A, top), which produces a hypomorphic allele that significantly reduces *DKC1* transcript levels (Figure 1B). The same mutation in the putative Sp1 transcription binding sites within the *DKC1* promoter has been previously reported (Knight et al., 2001; Salowsky et al., 2002). This patient presented at 2 years of age with several clinical features of DC including hematological defects, congenital anomalies involving the central nervous system and genitourinary system, and a family history of early-onset colon and lung cancers (Figure 1A, bottom). Therefore, *DKC1* (c.−141 C>G) cells provide a very unique system for assessing the impact of reducing the overall threshold of dyskerin activity.

We directly assessed the expression of functionally distinct H/ACA small RNAs in *DKC1*(c. −141 C>G) $CD34^+$ cells, including 27 H/ACA snoRNAs, which are the most abundant class of dyskerin-associated small RNAs involved in site-specific rRNA pseudouridylation (Figure 1C, top row). In addition, the expression of small Cajal body RNAs (scaRNAs), involved in pseudouridylation of spliceosomal small nuclear RNAs (snRNAs) (ACA12, U85, U93, and U109), as well as TERC, important for telomere function, were also examined. Unexpectedly, we observed differential reductions in the expression of distinct H/ACA small RNAs relative to matched healthy control $CD34^+$ cells (Figure 1C, top row), which did not display significant variations in H/ACA small RNA levels (Figure S1A; Table S1). Notably, the expression of H/ACA snoRNA15 and snoRNA67, which guide site-specific modifications of two consecutive Ψ residues on 18S rRNA (i.e., Ψ1367 and Ψ1445), displayed the greatest reduction, up to a 60% decrease (Figure 1C; Table S2). Interestingly, the levels of TERC remained unchanged in *DKC1*(c.–141 C>G) patient cells (Figure 1C; Table S2), and consistently no significant difference in telomere length was observed (Figure S2). These results suggest that missense mutations in *DKC1* have a more profound effect on TERC levels (Batista et al., 2011; Walne et al., 2007) as compared to the *DKC1* promoter mutation described in this study. For example, it is possible that missense mutations in dyskerin may disrupt specific protein-protein interactions within the telomerase complex that may be important for TERC stability. Nevertheless, these results indicate that distinct classes of dyskerin-associated H/ACA small RNAs may be differentially affected by this specific *DKC1* mutation.

In order to determine whether aberrant expression of H/ACA small RNAs is common among X-DC patients, we next extended our analysis to individuals harboring different *DKC1* mutations. In this respect, we performed unsupervised hierarchical clustering of H/ACA small RNA relative expression in *DKC1*(c.–141 C>G), *DKC1*(T66A), *DKC1*(ΔL37), and *DKC1*(A386T) patient cells (Figure 1C). We observed remarkable heterogeneity in the expression of H/ACA small RNAs among X-DC patient cells harboring different mutations that have similar histologic origins, relative to matched controls, which did not display significant variations in H/ACA small RNA levels (Figures S1B and S1C; Table S2). Moreover, specific H/ACA small RNAs stratified according to their relative expression levels, cell type, and nature of the *DKC1* mutation (Figure 1C, dendrograms). For example, the expression of a group of four H/ACA snoRNAs (snoRNA48, E2, 22, and 75) is perturbed in *DKC1*(ΔL37) fibroblasts but remains unaltered in *DKC1*(A386T) fibroblasts (Figure 1C; Table S2). Similar variations in the expression of distinct H/ACA small RNAs were also observed among X-DC patient lymphoblasts harboring different *DKC1* mutations (Figure 1C; Table S2). Furthermore, we also identified differences in H/ACA snoRNA expression in cells from different tissues (lymphoblasts versus fibroblasts) harboring the same *DKC1*(ΔL37) mutation (e.g., snoRNA31, 42, 15, and U85) (Figure 1C), suggesting that tissue-specific defects in H/ACA small RNA expression may at least in part underlie the specific pathological features present in X-DC patients. Common nodes of dysregulation in H/ACA small RNA expression are also evident. For example, six H/ACA small RNAs (snoRNA16, 52, 24, U93, ACA12, and TERC) display the most dramatic reductions in the majority of X-DC patient cells analyzed (Figure 1C). Moreover, we confirmed these findings by northern blot analysis (Figure S1D). Importantly, not all of the H/ACA small RNAs are reduced in X-DC patient cells. In particular, H/ACA snoRNAs such as 28 and U64 do not display differences in expression levels, in agreement with previous reports (Figure 1C; Table S2) (Batista et al., 2011; Mitchell et al., 1999). Interestingly, our observation that snoRNA42 expression is increased in *DKC1*(ΔL37) lymphocytes raises the possibility that certain snoRNAs may be selectively increased as a compensatory mechanism for perturbations in

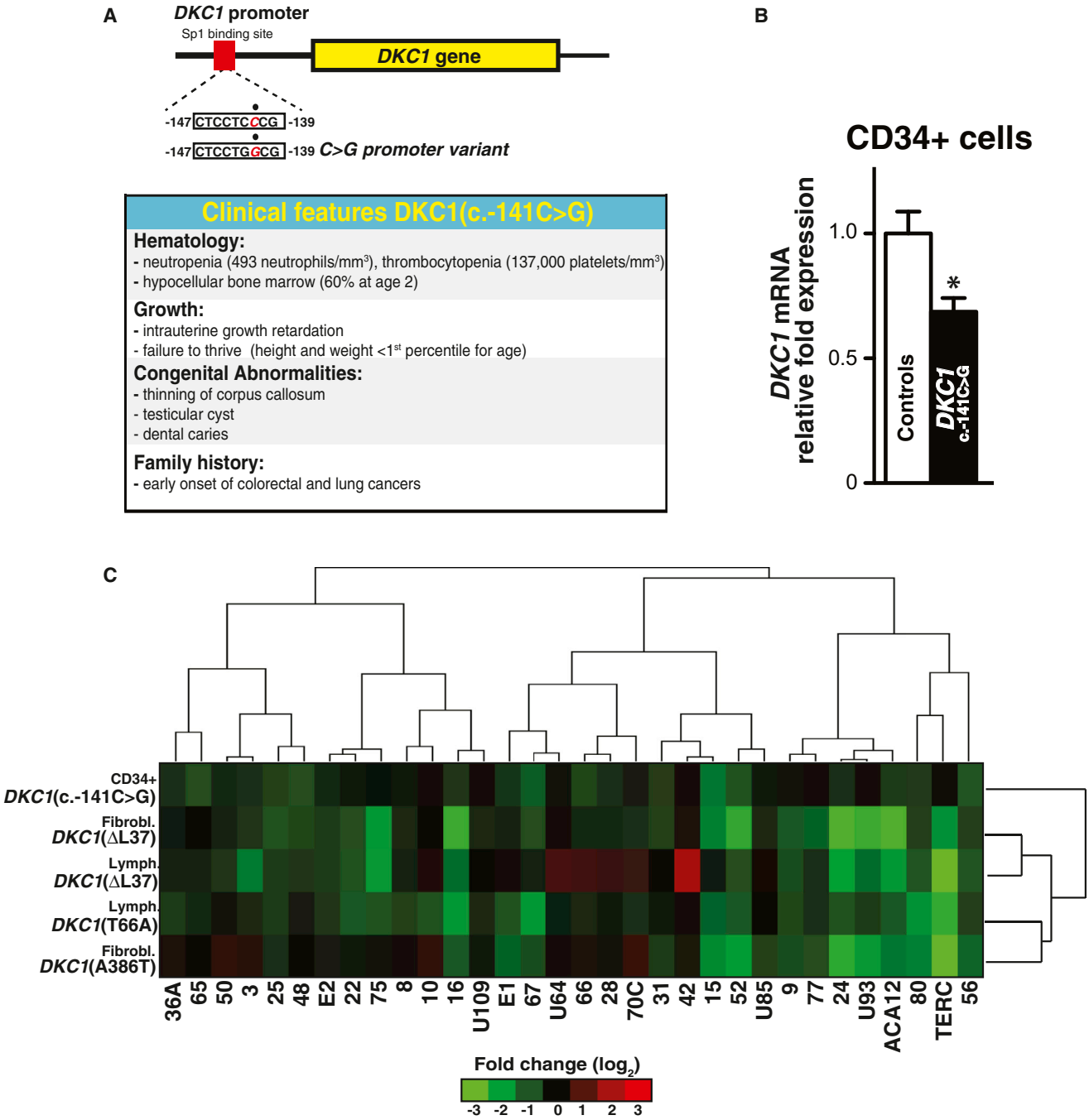

Figure 1. Characterization of Dyskerin-Associated H/ACA Small RNAs in X-DC Patient Cells

(A) Schematic of the *DKC1*(c.–141 C>G) mutation illustrating the position of the base-pair substitution on the *DKC1* promoter (top). Clinical features of the *DKC1*(c.–141 C>G) patient are listed (bottom).

(B) Quantification of *DKC1* messenger RNA (mRNA) levels in $CD34^+$ cells from two healthy controls and a *DKC1*(c.–141 C > G) patient was measured by real-time quantitative PCR (qPCR). Graphs show mean *DKC1* mRNA relative expression ±SEM in controls and *DKC1*(c.–141 C>G) $CD34^+$ cells.

(C) Heatmap diagram displaying hierarchical clustering of 32 H/ACA small RNA relative expression levels in X-DC patient cells. The expression of H/ACA small RNAs was measured by real-time qPCR, relative to two type-matched control cells for each mutation, and normalized to the abundance of RN7SK small noncoding RNA from at least three independent experiments. Each row represents a different type of X-DC patient-derived cell. Each column illustrates the expression of individual H/ACA small RNAs relative to controls. The color bar indicates the color-coding of small RNA expression from +3 to −3 in $\log_2$ space (bottom). Only slight variation in the expression of H/ACA small RNAs was observed among controls either by real-time qPCR or northern blot analysis (Figure S1; Tables S1 and S2). Statistical information is included in Table S2.

See also Figures S1 and S2 and Tables S1, S2, and S4.

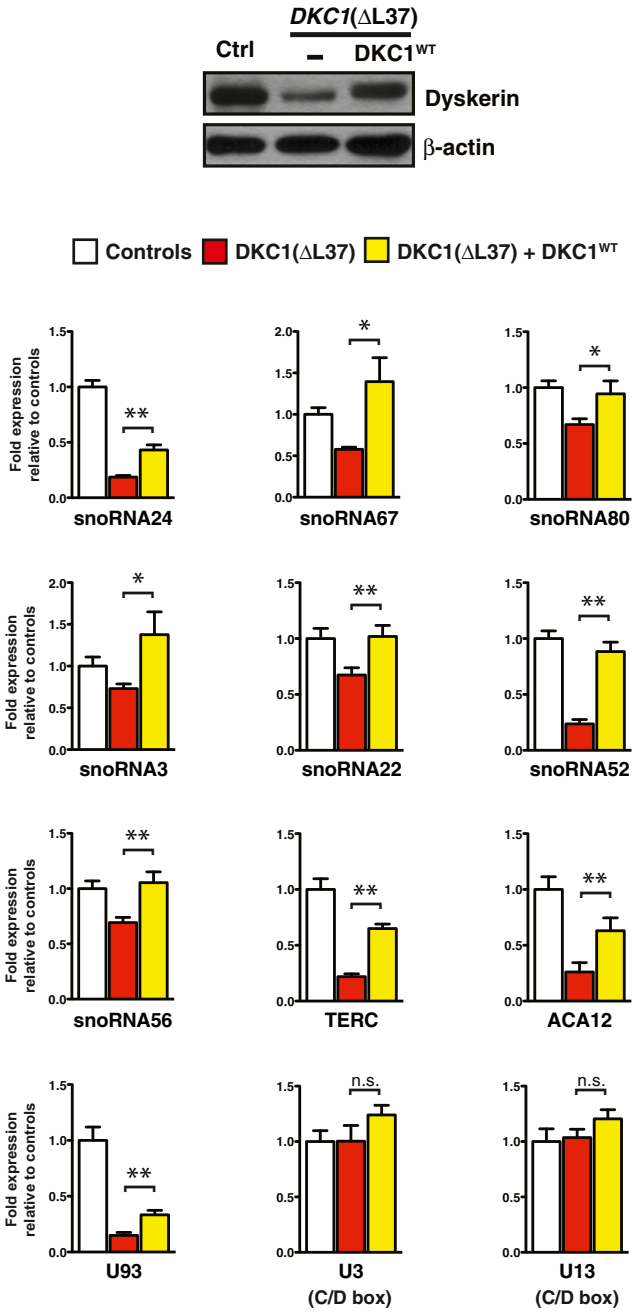

Figure 2. Expression of Dyskerin Rescues H/ACA Small RNA Expression Levels in Primary X-DC Fibroblasts

Expression levels of different classes of small RNAs in control, *DKC1*(ΔL37) primary fibroblasts, and *DKC1*(ΔL37) primary fibroblasts expressing exogenous wild-type dyskerin (DKC1^{WT}) measured by real-time qPCR. Graphs show mean fold expression ±SEM relative to control and normalized to the abundance of RN7SK small noncoding RNA from three independent experiments. Western blot analysis of dyskerin expression is shown in control and *DKC1*(ΔL37) primary fibroblasts in the absence or presence of DKC1^{WT} (top). β-actin was used as loading control. Statistical analysis was performed using the unpaired Student's t test (*$p < 0.05$ and **$p < 0.01$).

See also Table S4.

subsets of H/ACA small RNAs (Figure 1C). Strikingly, H/ACA sno/scaRNAs 24, U93, ACA12, 80, and 56 are decreased in the majority of X-DC patient cells, closely clustering with concomitant diminished TERC expression, and may therefore represent a central node of small RNA dysfunctions in human disease (Figure 1C). Importantly, the altered expression of H/ACA small RNAs in X-DC patients is highly specific, as a similar class of non-dyskerin-associated small RNAs implicated in methyl modifications of rRNA, termed C/D snoRNAs (Bachellerie and Cavaillé, 1997), are unaffected in X-DC patient cells (Figure 2; Table S2).

To establish whether the specific pattern of reductions in H/ACA small RNAs in X-DC cells is directly caused by dyskerin dysfunction, we restored dyskerin expression to near normal levels in primary X-DC fibroblasts (Figure 2). Importantly, reintroduction of dyskerin specifically rescued, to a large extent, the expression of dyskerin-associated H/ACA small RNAs in *DKC1*(ΔL37) primary fibroblasts compared to controls (Figure 2). Taken together, these results uncover aberrant expression of functionally diverse classes of dyskerin-associated H/ACA small RNAs in patients harboring distinct *DKC1* mutations. Furthermore, these findings suggest that variations in the expression of specific H/ACA small RNAs may underlie, at least in part, the wide range and degree of clinical features observed among X-DC patients.

Defects in Site-Specific and Global rRNA Pseudouridylation Are Present in X-DC Patients

Currently, it remains unknown whether dysregulations in H/ACA small RNA expression alter specific cellular processes orchestrated by these small RNAs. In particular, H/ACA snoRNAs are assembled into catalytically active RNP complexes through their association with dyskerin, which catalyzes the conversion of ~100 uridine residues to Ψ in functionally important domains of rRNA (Ni et al., 1997). To ascertain the contribution of altered H/ACA snoRNA expression in X-DC patient cells on Ψ modifications at specific sites on the rRNA, we developed a highly sensitive mass spectrometry method for relative quantification of changes in Ψ residues on rRNA at nucleotide resolution (see Figure 3A and Experimental Procedures for details). This technology enables quantification of site-specific pseudouridine modifications on individual rRNA nucleotides. In this study, we employed this technique to monitor the levels of site-specific Ψ modifications on 18S rRNA, as translational impairments upon dyskerin dysfunction are also associated with defects involving the preinitiation complex of translation (Bellodi et al., 2010b; Jack et al., 2011). Total 18S rRNA isolated from control and X-DC patient cells was cleaved to generate a mixture of Ψ-containing rRNA oligonucleotides that were subsequently resolved by liquid chromatography-tandem mass spectrometry (LC-MS/MS). Briefly, Ψ modifications at specific sites on rRNA oligonucleotides (Figure S3A and Table S3) were selected based on their *m/z* ratio and nucleotide sequence. The Ψ signal on each oligonucleotide was quantified and standardized to the amount of a non-Ψ-containing oligonucleotide in the mixture (see Experimental Procedures for details). In particular, we employed two distinct X-DC patient cells: *DKC1*(ΔL37) primary fibroblasts and immortalized *DKC1*(T66A) lymphoblasts.

Utilizing this methodology, we detected reductions in the amount of Ψ residues at specific sites on rRNA in these X-DC patient cells (Figure 3B), which precisely correspond to reductions in H/ACA snoRNAs annotated to guide these modifications (Figure S3A) (Lestrade and Weber, 2006). For example, in *DKC1*(ΔL37) fibroblasts, pronounced reductions were observed in Ψ levels at Ψ119, Ψ1367, and Ψ1445 on 18S rRNA compared to control cells (Figure 3B; Figure S3B). Conversely, no significant changes were detected at Ψ105 on 18S rRNA, in agreement with our findings that the expression of the corresponding guide H/ACA snoRNAs, 36A and 50, were not perturbed (Figure 1C; Table S2). In *DKC1*(T66A) cells, heterogeneous defects in site-specific pseudouridylation on 18S rRNA (Figure 3B; Figure S3C) were also observed, including perturbations in sites that were either reduced or unaltered in *DKC1*(ΔL37) fibroblasts. For example, Ψ1445 on 18S rRNA is similarly reduced in both *DKC1*(ΔL37) and *DKC1*(T66A) cells, and this is consistent with decreased expression of the corresponding guide H/ACA snoRNA (snoRNA67) in both cell types (Figures 1C and 3B). By contrast, the site-specific reductions of Ψ105, Ψ1692, or Ψ218 are exclusively observed in either *DKC1*(T66A) or *DKC1*(ΔL37) cells, respectively (Figures 3B and 3C). Based on these findings, we have uncovered a direct role for impaired H/ACA snoRNA expression toward defective patterns of rRNA pseudouridylation in X-DC patient cells. We further confirmed these findings by performing quantitative high-performance liquid chromatography (HPLC). Early-passage *DKC1*(ΔL37) primary fibroblasts displayed significant reductions in total pseudouridine levels in both 18S and 28S rRNA (Figure 3D). Notably, no differences in the total amount of 18S or 28S rRNA were observed (data not shown). Moreover, significant reductions in the total pseudouridine levels from five different *DKC1* point mutations including *DKC1*(T70I), *DKC1*(K314R), *DKC1*(K390Q), *DKC1*(A353V), and *DKC1*(T66A) were also observed (Figure 3E). The reductions in the total amount of rRNA pseudouridylation ranging from 10%–25% may reflect unique differences in specific patterns of modifications on rRNA as revealed by mass spectrometry. Together, these findings provide evidence that rRNA modification defects are common among X-DC patients. Moreover, the patterns of Ψ modifications are distinct and directly correlate with specific decreases in subsets of H/ACA snoRNAs originating from different *DKC1* point mutations.

The Pseudouridine Synthase Capacity of Dyskerin Is Important for Hematopoietic Stem Cell Function

As individual H/ACA small RNAs from diverse classes, including those implicated in ribosome, splicing, and telomerase functions, are altered in X-DC patient cells, an outstanding question is whether impaired dyskerin enzymatic activity is required for some of the pathological features of the disease. This is an important question, as dyskerin is able to associate with diverse H/ACA small RNAs to maintain their stability. However, dyskerin acts as a pseudouridine synthase in the context of only a subset of these small RNAs. For example, dyskerin's association with TERC serves to stabilize the telomerase complex; however, its association with H/ACA scaRNAs and snoRNAs converts these RNP particles into catalytically active complexes guiding site-specific conversions of uridine to Ψ residues on snRNA and rRNA, respectively (Meier, 2005). Given that bone marrow abnormalities are common and among the primary causes of early mortality in DC patients, we sought to determine the precise contribution of the pseudouridine synthase activity of dyskerin toward hematopoiesis. To this end, we employed *DKC1*(c.–141 C>G) primary $CD34^+$ hematopoietic progenitor cells. The *DKC1*(c.–141 C>G) mutation is characterized by severe features of X-DC, including significant bone marrow hypoplasia and cytopenia (Figure 1A). We introduced expression constructs for wild-type *DKC1* (designated $DKC1^{WT}$) or a catalytically inactive *DKC1* mutant, D125A (designated $DKC1^{D125A}$) so that they were both expressed at equivalent levels in *DKC1*(c.–141 C>G) $CD34^+$ cells (Figures S4A and S4B). $DKC1^{D125A}$ harbors a mutation in a critical amino acid within the evolutionarily conserved TruB Ψ synthase domain that is essential for enzymatic activity (Figure 4A; Figures S4C and S4D) (Hamma et al., 2005; Rashid et al., 2006; Zebarjadian et al., 1999). We next assessed hematopoietic progenitor colony formation on methylcellulose in the presence of a complete cocktail of cytokines that sustains the differentiation of progenitor cells into mature myeloid and erythroid cells (Figure 4B). *DKC1*(c.–141 C>G) $CD34^+$ cells are greatly impaired in their capacity to differentiate and generate mature myeloid and erythroid colonies as compared to matched healthy human $CD34^+$ cells (Figure 4B). Strikingly, the expression of $DKC1^{WT}$ completely restored the ability of *DKC1*(c.–141 C>G) $CD34^+$ progenitors to differentiate into mature myeloid and erythroid cells (Figure 4B). In contrast, introduction of the $DKC1^{D125A}$ catalytic mutant failed to rescue the severe differentiation defect present in these cells (Figure 4B). These findings provide significant insight into the molecular basis that may account for specific hematopoietic defects in X-DC patients and strongly implicate dyskerin's pseudouridine synthase enzymatic activity as a requirement for efficient hematopoiesis.

DISCUSSION

There is a growing realization that the majority of the human genome previously thought to be "junk DNA" encodes both short and long ncRNAs, which may instead exert important RNA-based cellular functions. However, the relative contribution of these RNAs to human disease is poorly understood. Our studies reveal that a large class of H/ACA small RNAs are found deregulated in human disease, displaying variable expression patterns that may dictate the number and the severity of disease features. With respect to H/ACA snoRNAs, deregulations in their expression patterns in X-DC directly produce site-specific defects in RNA modifications present on the ribosome, as revealed by state-of-the-art mass spectrometry. These findings provide a functional link between variations in expression patterns of H/ACA snoRNAs in disease and specific alterations in the array of nucleotide modifications present on the ribosome. Moreover, these studies suggest that heterogeneous pools of ribosomes harboring unique differences in modification patterns are present in X-DC patient cells. This heterogeneity in rRNA modifications may have important functional implications for expression of the X-DC patient genome at the posttranscriptional level and is consistent with previous studies revealing molecular

Cell PRESS
Open ACCESS

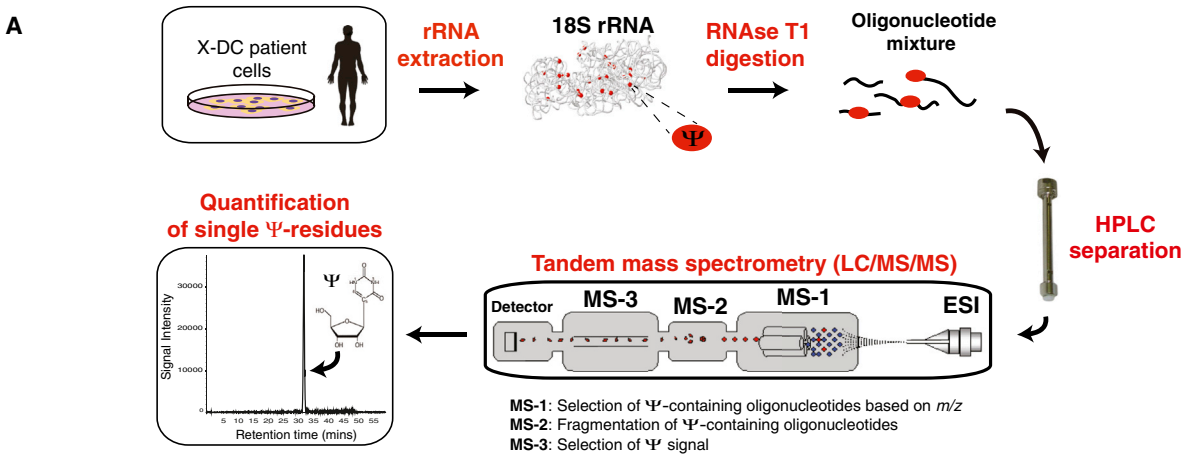

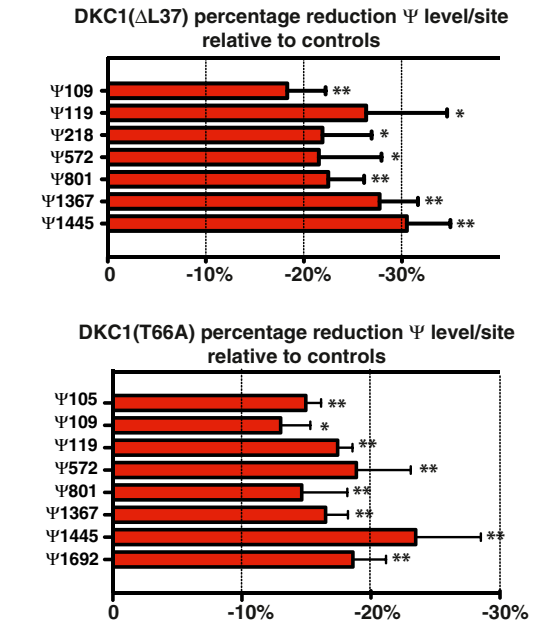

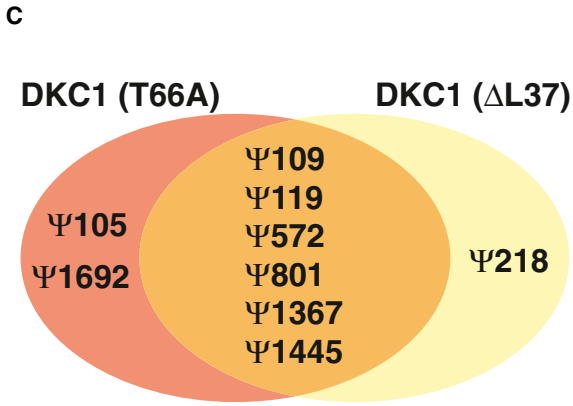

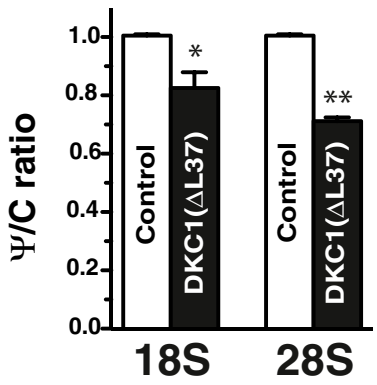

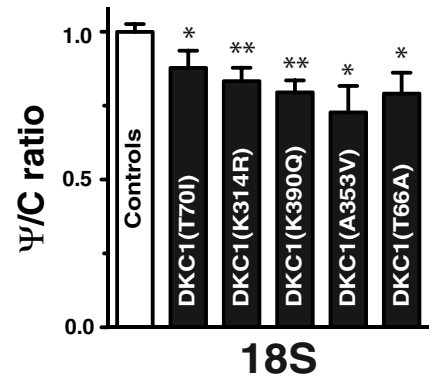

(legend on next page)

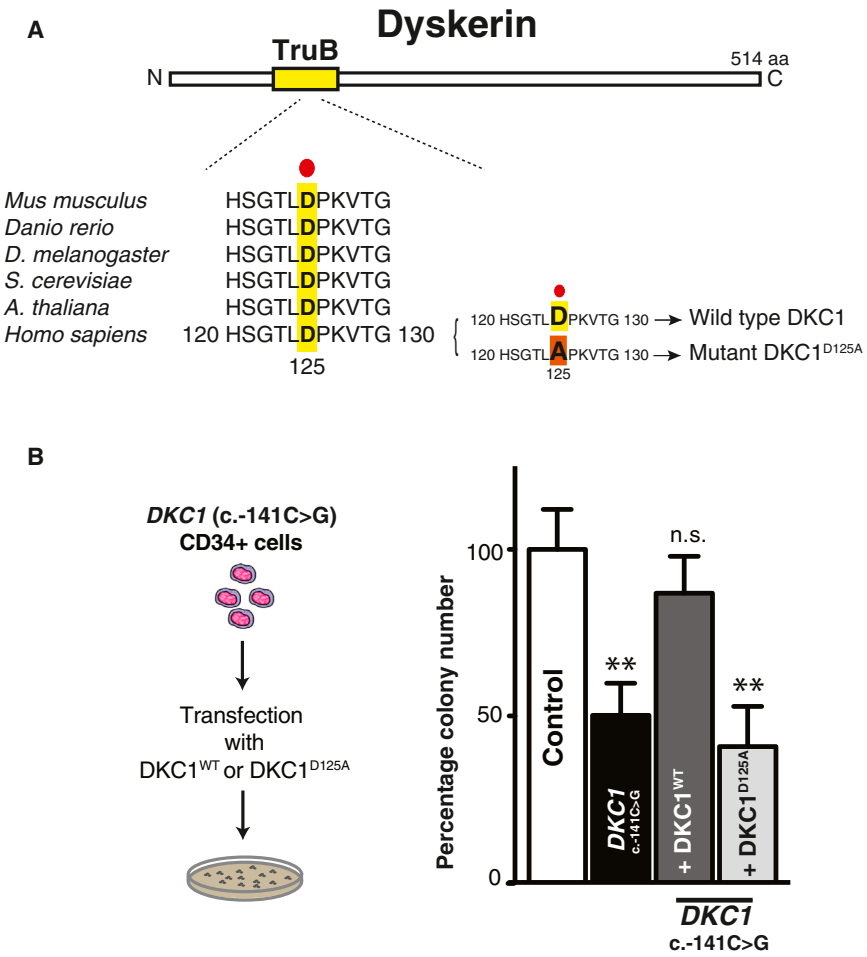

Figure 4. Dyskerin Pseudouridylation Activity Is Important for HSC Differentiation

(A) Schematic presentation of a dyskerin coding region highlighting the evolutionary conservation of the TruB Ψ synthase domain across several species. A substitution of aspartic acid (D) with alanine (A) at position 125 abolishes dyskerin pseudouridylation activity and was employed as a catalytically inactive DKC1$^{(D125A)}$ mutant.

(B) A hematopoietic colony-forming assay was performed on CD34^{+} progenitor cells from a healthy control and *DKC1*(c.–141 C>G) patient in the absence or presence of wild-type DKC1^{WT} or its catalytic mutant DKC1^{D125A} using methylcellulose supplemented with complete cytokines cocktail sustaining the growth of all blood cell lineages. The total number of colonies formed was scored 10 days after plating. Graph shows the mean total percentage number of colonies ±SEM relative to controls from two independent experiments. Statistical analysis was performed using the unpaired Student's t test (**$p < 0.01$).

See also Figure S4.

impairments in accurate translational control in X-DC patient cells (Bellodi et al., 2010a; Yoon et al., 2006). Moreover, a specific subgroup of H/ACA snoRNAs is commonly reduced among all *DKC1* patient mutations. Intriguingly, these H/ACA snoRNAs guide modifications that cluster primarily within two defined regions of the ribosome (Piekna-Przybylska et al., 2008), including expansion segment 6 (ES6) on 18S rRNA and domain II of 28S rRNA. These findings suggest that additional levels of specificity may coordinate the assembly of specific subsets of H/ACA snoRNPs required for modifications that cluster within functional regions of rRNA and are commonly deregulated in X-DC. Moreover, the mass spectrometry approach we have developed will now make it possible to test the intriguing possibility that different patterns of rRNA pseudouridylation may serve as a mechanism to modulate ribosome function in a cell-type- and tissue-specific manner.

Our study further reveals an important contribution of the pseudouridine synthase activity of dyskerin in hematopoiesis, which is critically impaired in X-DC patients (Dokal, 2000). This suggests a critical requirement for modifications of specific noncoding RNA species in accurate stem cell activity. This is further supported by the diminished expression of H/ACA snoRNAs, which require the catalytic activity of dyskerin.

Figure 3. Defective Site-Specific and Global rRNA Pseudouridylation Manifest in X-DC Patient Cells

(A) Schematic representation of the mass spectrometry approach used to detect site-specific pseudouridine modifications on 18S rRNA from control and X-DC patient cells. ESI, electrospray ionization; *m/z*, mass-to-charge ratio.

(B) Site-specific quantification of Ψ levels in two controls and in *DKC1*(ΔL37) fibroblasts (top) and *DKC1*(T66A) lymphoblasts (bottom). Graph shows mean percentage Ψ reduction ±SEM relative to two controls at specific Ψ sites on 18S rRNA from three independent experiments. Quantification of all Ψ sites examined in this study is shown in Figures S3B and S3C. The accuracy of these measurements is well controlled for by performing calibration curves, demonstrating a linear response to different concentrations of synthetic Ψ-containing oligonucleotides within the range of Ψ values observed in patient samples (Figure S3D). The percentage reductions in Ψ measurements are relative and not absolute.

(C) Venn diagram illustrates unique and commonly reduced Ψ sites in X-DC patient cells analyzed.

(D) HPLC quantification of 18S and 28S rRNA Ψ levels in control and *DKC1*(ΔL37) primary fibroblasts. The graph shows mean Ψ to cytosine (Ψ/C) ratio ±SEM relative to controls from two independent experiments.

(E) HPLC quantification of 18S rRNA Ψ levels in six independent controls and five X-DC lymphoblast cell lines harboring distinct *DKC1* point mutations. The specific *DKC1* mutation is presented on each column. The graph shows mean Ψ to cytosine (Ψ/C) ratio ±SEM for each X-DC lymphoblast cell line relative to controls from at least three independent experiments. Statistical analysis was performed using the unpaired Student's t test (*$p < 0.05$ and **$p < 0.01$).

See also Figure S3 and Table S3.

Thus, in addition to impaired telomere maintenance through reductions in TERC expression (Mitchell et al., 1999), heterogeneity in the expression and function of several additional H/ACA small RNAs may cause molecular defects that contribute to X-DC. The analysis of specific subsets of H/ACA small RNAs, such as those identified in our study, may be of great medical importance as prognostic markers, especially as the genetic basis of approximately 50% of DC patients remains unknown (Dokal, 2011). Further evidence for small RNAs in the pathogenesis of DC is highlighted by recent findings that the gene product of *C16orf57,* mutated in autosomal recessive DC and additional inherited diseases including poikiloderma with neutropenia, is required for the 3′ end processing of spliceosomal U6 snRNA (Hilcenko et al., 2013; Mroczek et al., 2012; Walne et al., 2010). Intriguingly, hypermethylation of several H/ACA snoRNA loci including snoRNA70C, which our findings reveal is deregulated in X-DC cells, has been reported in solid tumors (Ferreira et al., 2012). Thereby, small ncRNAs such as H/ACA snoRNAs may serve as important molecular markers for human health and should therefore be widely examined at the genomic and expression level in disease pathogenesis.

Our findings suggest that a common feature of human disease may be the selective pressure for mutations in specific core components of RNP complexes that associate with a multitude of small RNAs. For example, dyskerin's interactions with small H/ACA RNAs link the activity of a single protein to hundreds of RNAs involved in splicing, telomere activity, and ribosome function (Meier, 2006). Therefore, *DKC1* mutations simultaneously affect the expression and function of multiple classes of dyskerin-associated H/ACA small RNAs (Figure 1C) at the nexus of diverse RNA-based cellular processes. Thereby, mutations in genes encoding proteins such as dyskerin may reflect a particular vulnerability to the underlying biology of small RNAs, contributing to human disease. An outstanding question is the molecular nature of the extreme variability in the phenotypic spectrum of *DKC1* point mutations that range from severe birth defects to bone marrow failure to cancer. Impaired modifications of distinct functional RNAs may represent an important, novel molecular mechanism underlying these specific pathological features.

EXPERIMENTAL PROCEDURES

NCI Participant Lymphocytes

The patients with T70I, K314R, A353V, and K390Q mutations in *DKC1* are participants in the institutional review boards (IRBs)-approved longitudinal cohort study at the National Cancer Institute (NCI) entitled "Etiologic Investigation of Cancer Susceptibility in Inherited Bone Marrow Failure Syndromes" (http://www.marrowfailure.cancer.gov; NCI 02-C-0052, ClinicalTrials.gov Identifier: NCT00027274; Alter et al., 2010). See the Extended Experimental Procedures for detailed methods.

Primary Bone Marrow Progenitor Cells

Informed consent was obtained from the *DKC1*(c.–141 C>G) patient in accordance with a human subjects study protocol approved by the IRBs of the Seattle Children's Hospital and Fred Hutchinson Cancer Research Center. Anonymous healthy control bone marrow cells were obtained from discarded bone marrow harvest screens as approved by the Fred Hutchinson Cancer Research Center IRB.

HPLC and Mass Spectrometry Quantification of Human rRNA Pseudouridylation

Global analysis of rRNA pseudouridine levels was performed by HPLC analysis on a C_{18} 250 × 4.6 mm (particle size 5 μm) reverse-phase HPLC column (Agilent) as previously described (Jack et al., 2011). For quantifications of site-specific Ψ modifications, all LC-MS/MS analyses were performed using an in-house packed capillary column (320 μm inner diameter × 150 mm length, packed with Jupiter 4 μm Phenomenex Proteo 90 A material). The solvents used were as described elsewhere (Apffel et al., 1997) with minor modifications. A stock solvent solution was made consisting of 460 ml HPLC grade water (Fisher Scientific), 42 ml 1,1,1,3,3,3-hexafluoro-2-propanol (Fluka), and 1.2 ml triethylamine (Pierce). Solvent A was prepared by diluting the stock 1:1 V:V with HPLC grade water. Solvent B was prepared by diluting the stock 1:1 V:V with HPLC-grade methanol (Fisher). The HPLC system consisted of an Eldex Micropro LC and a Dionex LC-Packings FAMOS auto sampler. The flow rate was 5 to 7 μl/min on a 45 min linear gradient from 0%–70% B. All samples and standards were dissolved in solvent A prior to injection. Selected Ψ sites on human 18S rRNA (Figure S3A) were determined by LC-MS/MS following RNase T1 (Roche) digestion using 10 U/μg gel-purified 18S rRNA (0.2–1.0 μg) in 10 mM Tris-HCl, 1 mM EDTA (pH 7.4) on a Thermo LTQ Orbitrap Velos mass spectrometer using 90 min gradients and operated in negative ion detection mode. The IS voltage was set at 4.0 to 5.0 kV, with source temperature at 225°C and a sheath gas flow of 10. The instrument was run in a data dependent mode, using a survey scan from 400 to 1,600, resolution 30,000, and with a 2E6 AGC setting for full scan with one microscan of 250 ms. After every survey scan, the top three most intense ions were selected for HCD fragmentation with 2E5 AGC setting, and 3 × 200 ms microscans. The HCD mass range was set at 100–2,000. Ions selected for HCD were added to an exclusion list for the next 60 s. The data files were processed using Xcalibur software suite (Thermo Scientific). Extracted ion profiles for previously characterized Ψ ions at 165.0302 (when the Ψ is at the 5′ end of an oligo) and 207.0400 (when elsewhere in the oligo) (Pomerantz and McCloskey, 2005) were created for all data files and were used to locate and map distinct Ψ-containing oligonucleotides from purified human 18S rRNA. The HCD spectrum was manually interpreted with the aid of Ariadne (Nakayama et al., 2009) and the Mongo Oligo Mass Calculator program (http://rna-mdb.cas.albany.edu/RNAmods/masspec/mongo.htm). The identifications of Ψ-containing oligonucleotides were facilitated by the accurate masses (±5 ppm) obtained from the Velos instrument in both full scan and HCD scan mode. The transitions used for MRM experiments and retention times for each oligonucleotide are shown in Table S3. See the Extended Experimental Procedures for detailed methods.

Western Blot, Northern Blot, and Quantitative PCR Analysis

Western blot was performed using standard protocols and the following primary antibodies: dyskerin (1:1,000; Santa Cruz), FLAG (1:1,000; Sigma-Aldrich), and β-actin (1: 5,000; Sigma-Aldrich). Northern blot analysis was performed on total RNA (2 μg), isolated with Trizol reagent (Invitrogen), using ^{32}P end-labeled oligonucleotides (Table S4), and quantification was performed using ImageQuant 5.2 software (Molecular Dynamics). The expression of H/ACA small RNAs was measured by real-time quantitative PCR (qPCR), relative to two type-matched control cells for each mutation, and normalized to the abundance of RN7SK small ncRNA from at least three independent experiments. Primer sequences are listed in Table S4.

Telomere Length Measurements

Telomere length was measured by multicolor flow FISH (Repeat Diagnostics) as described previously (Alter et al., 2007; Baerlocher et al., 2006).

SUPPLEMENTAL INFORMATION

Supplemental Information includes Extended Experimental Procedures, four figures, and four tables and can be found with this article online at http://dx.doi.org/10.1016/j.celrep.2013.04.030.

LICENSING INFORMATION

ACKNOWLEDGMENTS

We thank M. Barna for critical discussion and reading of this manuscript, K. Tong for editing the manuscript, the Fujimori laboratory for technical support and equipment, J. Johl for technical assistance, and Lizette Caballero and the UCSF BMT Laboratory for their generous assistance. We also thank Drs. B.P. Alter and N. Giri at the National Cancer Institute for clinical characterization of patients and biospecimen collection. We are grateful to the patients for their valuable contributions to this study. C.B. is a fellow of the Leukemia & Lymphoma Society and the Aplastic Anemia & MDS International Foundation. D.R. is a Leukemia & Lymphoma Society Scholar. This work was supported, in part, by the intramural research program of the Division of Cancer Epidemiology and Genetics, National Cancer Institute, National Institutes of Health (S.S.). This work is supported by NIH NIGMS 8P41GM103481 and Howard Hughes Medical Institute (A.B.), NIH R01DK098057 (D.R.), NIH R01HL085572 (D.R.), and NIH 3R01HL085572-05S1 (D.R.).

Received: January 4, 2013
Revised: March 29, 2013
Accepted: April 24, 2013
Published: May 23, 2013

REFERENCES

Alter, B.P., Baerlocher, G.M., Savage, S.A., Chanock, S.J., Weksler, B.B., Willner, J.P., Peters, J.A., Giri, N., and Lansdorp, P.M. (2007). Very short telomere length by flow fluorescence in situ hybridization identifies patients with dyskeratosis congenita. Blood *110*, 1439–1447.

Alter, B.P., Giri, N., Savage, S.A., Peters, J.A., Loud, J.T., Leathwood, L., Carr, A.G., Greene, M.H., and Rosenberg, P.S. (2010). Malignancies and survival patterns in the National Cancer Institute inherited bone marrow failure syndromes cohort study. Br. J. Haematol. *150*, 179–188.

Apffel, A., Chakel, J.A., Fischer, S., Lichtenwalter, K., and Hancock, W.S. (1997). Analysis of Oligonucleotides by HPLC-Electrospray Ionization Mass Spectrometry. Anal. Chem. *69*, 1320–1325.

Bachellerie, J.P., and Cavaillé, J. (1997). Guiding ribose methylation of rRNA. Trends Biochem. Sci. *22*, 257–261.

Baerlocher, G.M., Vulto, I., de Jong, G., and Lansdorp, P.M. (2006). Flow cytometry and FISH to measure the average length of telomeres (flow FISH). Nat. Protoc. *1*, 2365–2376.

Batista, L.F., Pech, M.F., Zhong, F.L., Nguyen, H.N., Xie, K.T., Zaug, A.J., Crary, S.M., Choi, J., Sebastiano, V., Cherry, A., et al. (2011). Telomere shortening and loss of self-renewal in dyskeratosis congenita induced pluripotent stem cells. Nature *474*, 399–402.

Baxter-Roshek, J.L., Petrov, A.N., and Dinman, J.D. (2007). Optimization of ribosome structure and function by rRNA base modification. PLoS ONE *2*, e174.

Bellodi, C., Kopmar, N., and Ruggero, D. (2010a). Deregulation of oncogene-induced senescence and p53 translational control in X-linked dyskeratosis congenita. EMBO J. *29*, 1865–1876.

Bellodi, C., Krasnykh, O., Haynes, N., Theodoropoulou, M., Peng, G., Montanaro, L., and Ruggero, D. (2010b). Loss of function of the tumor suppressor DKC1 perturbs p27 translation control and contributes to pituitary tumorigenesis. Cancer Res. *70*, 6026–6035.

Cerami, E., Gao, J., Dogrusoz, U., Gross, B.E., Sumer, S.O., Aksoy, B.A., Jacobsen, A., Byrne, C.J., Heuer, M.L., Larsson, E., et al. (2012). The cBio cancer genomics portal: an open platform for exploring multidimensional cancer genomics data. Cancer Discov. *2*, 401–404.

Charette, M., and Gray, M.W. (2000). Pseudouridine in RNA: what, where, how, and why. IUBMB Life *49*, 341–351.

Dokal, I. (2000). Dyskeratosis congenita in all its forms. Br. J. Haematol. *110*, 768–779.

Dokal, I. (2011). Dyskeratosis congenita. Hematology Am. Soc. Hematol. Educ. Program *2011*, 480–486.

Ferreira, H.J., Heyn, H., Moutinho, C., and Esteller, M. (2012). CpG island hypermethylation-associated silencing of small nucleolar RNAs in human cancer. RNA Biol. *9*, 881–890.

Forbes, S.A., Bindal, N., Bamford, S., Cole, C., Kok, C.Y., Beare, D., Jia, M., Shepherd, R., Leung, K., Menzies, A., et al. (2011). COSMIC: mining complete cancer genomes in the Catalogue of Somatic Mutations in Cancer. Nucleic Acids Res. *39*(Database issue), D945–D950.

Hamma, T., Reichow, S.L., Varani, G., and Ferré-D'Amaré, A.R. (2005). The Cbf5-Nop10 complex is a molecular bracket that organizes box H/ACA RNPs. Nat. Struct. Mol. Biol. *12*, 1101–1107.

Heiss, N.S., Knight, S.W., Vulliamy, T.J., Klauck, S.M., Wiemann, S., Mason, P.J., Poustka, A., and Dokal, I. (1998). X-linked dyskeratosis congenita is caused by mutations in a highly conserved gene with putative nucleolar functions. Nat. Genet. *19*, 32–38.

Hilcenko, C., Simpson, P.J., Finch, A.J., Bowler, F.R., Churcher, M.J., Jin, L., Packman, L.C., Shlien, A., Campbell, P., Kirwan, M., et al. (2013). Aberrant 3′ oligoadenylation of spliceosomal U6 small nuclear RNA in poikiloderma with neutropenia. Blood *121*, 1028–1038.

Jack, K., Bellodi, C., Landry, D.M., Niederer, R.O., Meskauskas, A., Musalgaonkar, S., Kopmar, N., Krasnykh, O., Dean, A.M., Thompson, S.R., et al. (2011). rRNA pseudouridylation defects affect ribosomal ligand binding and translational fidelity from yeast to human cells. Mol. Cell *44*, 660–666.

Kirwan, M., and Dokal, I. (2008). Dyskeratosis congenita: a genetic disorder of many faces. Clin. Genet. *73*, 103–112.

Knight, S.W., Heiss, N.S., Vulliamy, T.J., Aalfs, C.M., McMahon, C., Richmond, P., Jones, A., Hennekam, R.C., Poustka, A., Mason, P.J., and Dokal, I. (1999). Unexplained aplastic anaemia, immunodeficiency, and cerebellar hypoplasia (Hoyeraal-Hreidarsson syndrome) due to mutations in the dyskeratosis congenita gene, DKC1. Br. J. Haematol. *107*, 335–339.

Knight, S.W., Vulliamy, T.J., Morgan, B., Devriendt, K., Mason, P.J., and Dokal, I. (2001). Identification of novel DKC1 mutations in patients with dyskeratosis congenita: implications for pathophysiology and diagnosis. Hum. Genet. *108*, 299–303.

Lafontaine, D.L., Bousquet-Antonelli, C., Henry, Y., Caizergues-Ferrer, M., and Tollervey, D. (1998). The box H + ACA snoRNAs carry Cbf5p, the putative rRNA pseudouridine synthase. Genes Dev. *12*, 527–537.

Lestrade, L., and Weber, M.J. (2006). snoRNA-LBME-db, a comprehensive database of human H/ACA and C/D box snoRNAs. Nucleic Acids Res. *34*(Database issue), D158–D162.

Matera, A.G., Terns, R.M., and Terns, M.P. (2007). Non-coding RNAs: lessons from the small nuclear and small nucleolar RNAs. Nat. Rev. Mol. Cell Biol. *8*, 209–220.

Meier, U.T. (2005). The many facets of H/ACA ribonucleoproteins. Chromosoma *114*, 1–14.

Meier, U.T. (2006). How a single protein complex accommodates many different H/ACA RNAs. Trends Biochem. Sci. *31*, 311–315.

Mitchell, J.R., Wood, E., and Collins, K. (1999). A telomerase component is defective in the human disease dyskeratosis congenita. Nature *402*, 551–555.

Montanaro, L. (2010). Dyskerin and cancer: more than telomerase. The defect in mRNA translation helps in explaining how a proliferative defect leads to cancer. J. Pathol. *222*, 345–349.

Mroczek, S., Krwawicz, J., Kutner, J., Lazniewski, M., Kuciński, I., Ginalski, K., and Dziembowski, A. (2012). C16orf57, a gene mutated in poikiloderma with neutropenia, encodes a putative phosphodiesterase responsible for the U6 snRNA 3′ end modification. Genes Dev. *26*, 1911–1925.

Nakayama, H., Akiyama, M., Taoka, M., Yamauchi, Y., Nobe, Y., Ishikawa, H., Takahashi, N., and Isobe, T. (2009). Ariadne: a database search engine for identification and chemical analysis of RNA using tandem mass spectrometry data. Nucleic Acids Res. *37*, e47.

Ni, J., Tien, A.L., and Fournier, M.J. (1997). Small nucleolar RNAs direct site-specific synthesis of pseudouridine in ribosomal RNA. Cell *89*, 565–573.

Piekna-Przybylska, D., Decatur, W.A., and Fournier, M.J. (2008). The 3D rRNA modification maps database: with interactive tools for ribosome analysis. Nucleic Acids Res. *36*(Database issue), D178–D183.

Pomerantz, S.C., and McCloskey, J.A. (2005). Detection of the common RNA nucleoside pseudouridine in mixtures of oligonucleotides by mass spectrometry. Anal. Chem. *77*, 4687–4697.

Rashid, R., Liang, B., Baker, D.L., Youssef, O.A., He, Y., Phipps, K., Terns, R.M., Terns, M.P., and Li, H. (2006). Crystal structure of a Cbf5-Nop10-Gar1 complex and implications in RNA-guided pseudouridylation and dyskeratosis congenita. Mol. Cell *21*, 249–260.

Reichow, S.L., Hamma, T., Ferré-D'Amaré, A.R., and Varani, G. (2007). The structure and function of small nucleolar ribonucleoproteins. Nucleic Acids Res. *35*, 1452–1464.

Ronchetti, D., Todoerti, K., Tuana, G., Agnelli, L., Mosca, L., Lionetti, M., Fabris, S., Colapietro, P., Miozzo, M., Ferrarini, M., et al. (2012). The expression pattern of small nucleolar and small Cajal body-specific RNAs characterizes distinct molecular subtypes of multiple myeloma. Blood Cancer J. *2*, e96.

Salowsky, R., Heiss, N.S., Benner, A., Wittig, R., and Poustka, A. (2002). Basal transcription activity of the dyskeratosis congenita gene is mediated by Sp1 and Sp3 and a patient mutation in a Sp1 binding site is associated with decreased promoter activity. Gene *293*, 9–19.

Teittinen, K.J., Laiho, A., Uusimaki, A., Pursiheimo, J.P., Gyenesei, A., and Lohi, O. (2013). Expression of small nucleolar RNAs in leukemic cells. Cell Oncol. (Dordr). *36*, 55–63.

Valleron, W., Laprevotte, E., Gautier, E.F., Quelen, C., Demur, C., Delabesse, E., Agirre, X., Prosper, F., Kiss, T., and Brousset, P. (2012a). Specific small nucleolar RNA expression profiles in acute leukemia. Leukemia *26*, 2052–2060.

Valleron, W., Ysebaert, L., Berquet, L., Fataccioli, V., Quelen, C., Martin, A., Parrens, M., Lamant, L., de Leval, L., Gisselbrecht, C., et al. (2012b). Small nucleolar RNA expression profiling identifies potential prognostic markers in peripheral T-cell lymphoma. Blood *120*, 3997–4005.

Walne, A.J., Vulliamy, T., Marrone, A., Beswick, R., Kirwan, M., Masunari, Y., Al-Qurashi, F.H., Aljurf, M., and Dokal, I. (2007). Genetic heterogeneity in autosomal recessive dyskeratosis congenita with one subtype due to mutations in the telomerase-associated protein NOP10. Hum. Mol. Genet. *16*, 1619–1629.

Walne, A.J., Vulliamy, T., Beswick, R., Kirwan, M., and Dokal, I. (2010). Mutations in C16orf57 and normal-length telomeres unify a subset of patients with dyskeratosis congenita, poikiloderma with neutropenia and Rothmund-Thomson syndrome. Hum. Mol. Genet. *19*, 4453–4461.

Watkins, N.J., Gottschalk, A., Neubauer, G., Kastner, B., Fabrizio, P., Mann, M., and Lührmann, R. (1998). Cbf5p, a potential pseudouridine synthase, and Nhp2p, a putative RNA-binding protein, are present together with Gar1p in all H BOX/ACA-motif snoRNPs and constitute a common bipartite structure. RNA *4*, 1549–1568.

Williams, G.T., and Farzaneh, F. (2012). Are snoRNAs and snoRNA host genes new players in cancer? Nat. Rev. Cancer *12*, 84–88.

Yip, S., Butterfield, Y.S., Morozova, O., Chittaranjan, S., Blough, M.D., An, J., Birol, I., Chesnelong, C., Chiu, R., Chuah, E., et al. (2012). Concurrent CIC mutations, IDH mutations, and 1p/19q loss distinguish oligodendrogliomas from other cancers. J. Pathol. *226*, 7–16.

Yoon, A., Peng, G., Brandenburger, Y., Zollo, O., Xu, W., Rego, E., and Ruggero, D. (2006). Impaired control of IRES-mediated translation in X-linked dyskeratosis congenita. Science *312*, 902–906.

Zebarjadian, Y., King, T., Fournier, M.J., Clarke, L., and Carbon, J. (1999). Point mutations in yeast CBF5 can abolish in vivo pseudouridylation of rRNA. Mol. Cell. Biol. *19*, 7461–7472.